An Improved Reactive Power Sharing in an Isolated Microgrid with a Local Load Detection

*Issam A. Smadi** *and Luay I. Shehadeh*

(Department of Electrical Engineering, Jordan University of Science and Technology, Irbid 22110, Jordan)

Abstract: Accurate reactive power sharing is one of the main issues in isolated microgrids to avoid circulating currents and overloading small distributed generation (DG) units. A simple and enhanced method for improving reactive power sharing among parallel-connected DG systems in an isolated microgrid was proposed. The proposed method uses a compensator term with an integral action to minimize the reactive power-sharing error internally without any need for communication or information shared among the DG units. Moreover, a small disturbance carrying part of the reactive power-sharing error is injected into the active power-droop controller, maintaining the essential system parameters within their allowable limits. Consequently, a simple compensation trigger system is proposed to effectively detect any local load change in the network and provide compensation gains to activate the proposed control method. The stability of the proposed method was verified and analyzed using a detailed small-signal model. Moreover, the effectiveness and robustness of the proposed method were validated through comprehensive simulation studies and comparisons with other related techniques.

Keywords: Adaptive droop, distributed generation (DG), droop control, microgrid, power management, reactive power-sharing

1 Introduction

Currently, the application of distributed generators (DGs) is increasing significantly. DGs offer various advantages over conventional generation systems, such as less pollution, more flexible placement, a higher effective energy rate, and lower transmission power losses. Moreover, DGs provide greater controllability and operability than conventional generation systems. However, because most DG units interface with the grid using power electronic converters, some unwanted features have been introduced, such as system resonance and protection from interference. The concept of the microgrid (MG) has been proposed to overcome these problems [1-2].

MGs offer excellent power management, operability, and controllability in distributed networks. Furthermore, it operates in either a grid-connected or isolated mode and can economically benefit customers and utilities [3].

In isolated MGs, it is recommended that the loads be shared evenly by the connected DG units to avoid circulating currents among them. The droop control method is a well-known method used in MG to achieve power sharing among DG in a decentralized manner [4-6]. However, owing to the difference in DG locations, random size, placement of the loads among microgrid systems, and the impedance resistive nature of the feeder, the droop control method fails to achieve accurate reactive power-sharing [7-10].

Unequal reactive power sharing can overload smaller DG units closer to the heavier load and cause a circulating current and uneven voltage profile, which leads to incorrect protection system triggers and can result in system stability problems [11]. Therefore, several strategies and methods have been proposed to overcome the reactive power-sharing problem. These strategies are based on the concepts of virtual impedance [9, 11-16] and the droop control concept [17-26].

The virtual impedance technique reduces line impedance differences and enhances reactive power sharing, either with communication [11-13] or without [14-16]. Although this technique effectively provides accurate reactive power sharing, incorrect design of the virtual impedance affects the voltage profile and system stability. In Ref. [17], the effect of the line impedance on the power-sharing accuracy was

Manuscript received August 3, 2022; revised January 5, 2023; accepted February 11, 2023. Date of publication June 30, 2023; date of current version May 22, 2023.
* Corresponding Author, E-mail: iasmadi@just.edu.jo
Digital Object Identifier: 10.23919/CJEE.2023.000021

mitigated based on signal detection on the high-voltage side of the coupled transformer. However, this method is limited to high-voltage (HV)-MG applications.

Another way to minimize the reactive power-sharing error is to continually adjust the nominal voltage by linking it to the frequency based on a tuned parameter [18]. However, the method is inaccurate. Ref. [19] proposed an adaptive voltage droop scheme in which two terms are added to the conventional Q-V droop relation. The first term compensates for the voltage drop, and the second term improves reactive power sharing and system stability. However, this method requires knowledge of system parameters. In Ref. [20], an adaptive Q-V droop slope coefficient was proposed to improve reactive power sharing among DG units based on the transient energy concept. A Q-$\dot{V}$ droop for improving reactive power sharing was presented in Ref. [21]. This technique provides a trade-off between voltage regulation and reactive power-sharing improvement; accordingly, the system stability can be affected. A new perspective focusing on changing the voltage bias using two stages-error reduction and voltage recovery-was proposed in Ref. [22]. Thus, this method is effective and accurate. However, this requires a low-bandwidth communication link, and the design of the controller is not straightforward.

Another approach involves adding a small disturbance from the reactive power-sharing error to the P-ω droop relationship for each inverter. In Ref. [23], a low-bandwidth communication link simultaneously provides an occasional trigger from the central controller to all DG units. The response of active power to a small added disturbance is collected and compared with its average stored value before compensation. Subsequently, a correction signal is injected into the Q-V droop to mitigate the reactive power-sharing error. An enhancement to Ref. [23] is proposed in Ref. [24] by adding a partition of the reactive power-sharing error to the P-ω droop relationship for each inverter. This modification reduces the disturbance over the active power when compensation is initiated. However, these methods require a low-bandwidth communication link to commence the compensation process, and their stability is not guaranteed. In Ref. [25], a local load change detector was proposed to solve the need for a communication link to simultaneously initiate the compensation process for all DGs. However, this technique used the same controller as that used in Ref. [23], which requires additional components to be represented and, accordingly, is more complex. The authors in Ref. [26] attempted to enhance Ref. [23] by introducing a virtual synchronous generator (VSG) relation to solve the active power disturbance presented during the compensation process and, accordingly, to provide a regulation signal to the Q-V droop relation. Although this technique provides quick and effective regulation, it requires a communication signal from the center controller to commence the compensation process.

In addition to achieving accurate reactive power sharing, the controller should meet the desired characteristics, such as the plug-and-play features of the DG units, simple design, insensitivity to load changes, and avoidance of any communication links. This paper proposes an improved local controller to minimize the reactive power-sharing mismatch among DG units by changing the voltage bias based on conventional droop control. Communication from the central controller, measurements, or external information among the DG units is not required. The proposed method uses a simple and cost-effective approach to reduce the reactive power-sharing error locally activated by the proposed compensation trigger system. Simulation results are obtained to verify the effectiveness of the proposed strategy.

The remainder of this paper is organized as follows: Section 2 discusses conventional droop control. In Section 3, the proposed method is introduced and described in detail. A detailed small-signal analysis is presented in Section 4. A simulation analysis to verify the effectiveness of the proposed method is presented in Section 5. Finally, the conclusions are presented in Section 6.

2 Conventional droop control

The conventional droop control method is a well-known technique used in isolated MGs to achieve proportional power sharing by imitating the droop characteristics of a synchronous generator (SG) in a decentralized manner [4-5].

Conventional droop control was adopted based on the power flow through the transmission line. Fig. 1 shows the equivalent configuration of a DG unit through an isolated MG system. The output voltage from the DG is donated by $E_{DG}\angle\delta$, where δ is the power angle. The feeder impedance is $Z_i\angle\theta$, where θ is the impedance angle, and the voltage at the point of common coupling (PCC) is denoted as $V_{PCC}\angle 0^\circ$. The delivered active and reactive powers are coupled owing to the nature of the feeder impedance, which is almost inductive for medium- and high-voltage applications. Therefore, the feeder resistance can be neglected. Accordingly, the active and reactive droop relations can be expressed as

$$\omega = \omega_n - k_p P_f \tag{1}$$

$$E = E_n - k_q Q_f \tag{2}$$

where ω_n and E_n are the nominal angular frequency and voltage of the DG, respectively, at no load. k_p and k_q are the droop coefficients of the active and reactive droop relationships, respectively. P_f and Q_f are the active and reactive power values after low-pass filtering (LPF), respectively.

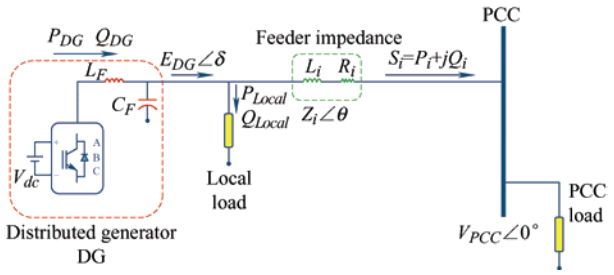

Fig. 1 Power flow in a simple microgrid configuration

To share the MG load power among the connected DG units in proportion to their power ratings, the droop slope coefficients k_p and k_q of the parallel-connected DG units should be designed to be inversely proportional to their power ratings [27]. Therefore, the conventional droop method can share active power evenly because the operating frequency is the same among the parallel-connected units in a steady state. However, the conventional droop method does not provide accurate reactive power sharing because of the voltage deviation among the DG units introduced by the differences in line impedance and placement of the DG units.

3 Proposed reactive power sharing method

3.1 Proposed control method

The proposed control method improves the reactive power sharing by introducing two terms to the conventional droop method during a short compensation duration. The first term is introduced to the Q-E droop relation to improve reactive power sharing. Meanwhile, the second term is introduced to the P-ω droop relation during compensation to provide short-term coupling between the P-ω and Q-E droop relations. The proposed control method is illustrated in Fig. 2 and is expressed as

$$E = E_n - k_q Q_f - k_c \int G Q_f \tag{3}$$

$$\omega = \omega_n - k_p P_f - k_s G Q_f \tag{4}$$

The last terms in Eq. (3) and Eq. (4) are the additional terms introduced by the proposed control method, where the compensation terms are k_c and k_s. G is the compensation gain, which is used to smoothly

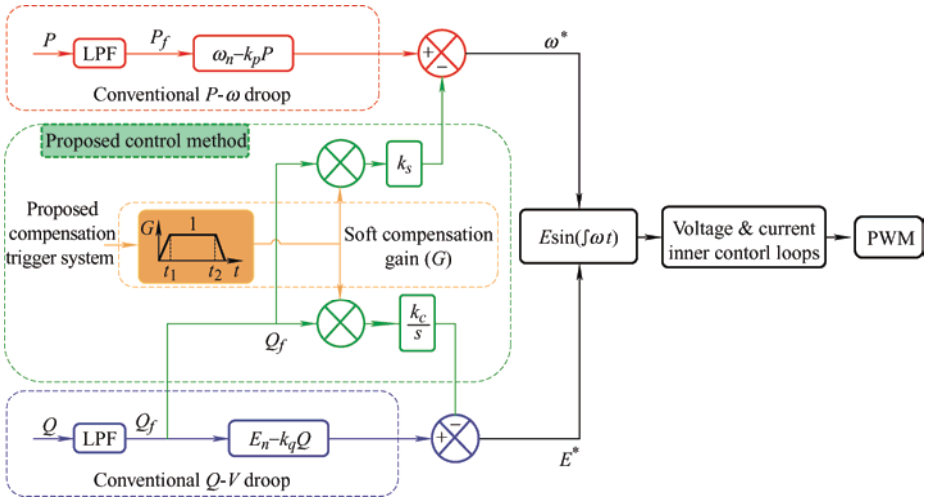

Fig. 2 Proposed reactive power-sharing error compensation method

trigger the proposed method during compensation.

To illustrate the process of the first term, if there are two parallelly connected DG units with the same power ratings controlled by the conventional droop control, there will be a mismatch in their shared reactive power owing to certain factors. For simplicity, the impact of the feeder reactance mismatch on reactive power sharing is shown in Fig. 3a. The relationship between the DG output reactive power and the magnitude difference between the PCC voltage and DG voltages, assuming DG feeder characteristics, is linear, as shown in Eq. (5). When compensation begins, a new term is introduced to the conventional *Q-E* droop relation that modifies the voltage bias of the connected DG units and regulates the reactive power-sharing error using a compensator and an integral action. Thus, the design of the first term is straightforward. Fig. 3b illustrates the process for the first term.

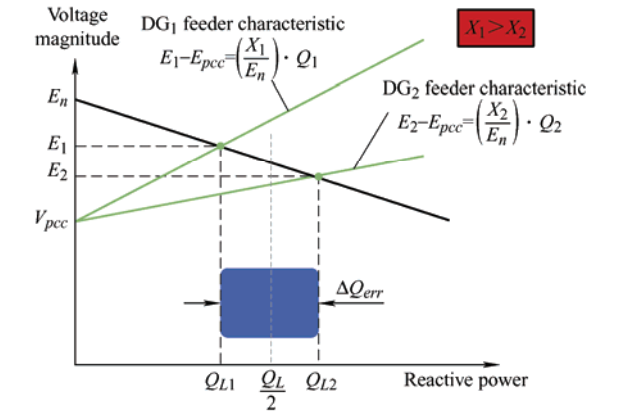

(a) Reactive power sharing of two DG units with unequal feeder reactance

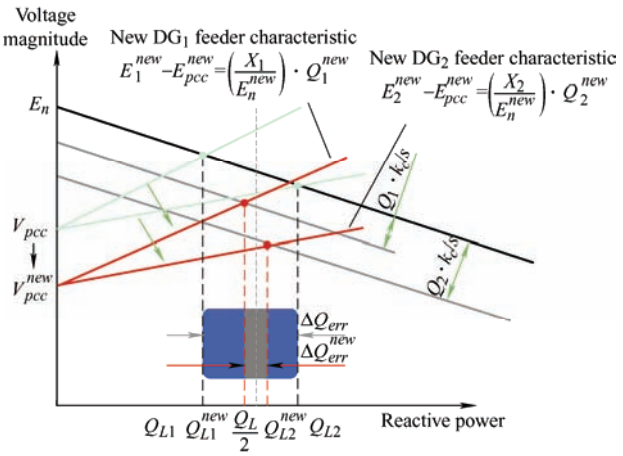

(b) Graphical representation of the first term

Fig. 3 Illustration of the first term of the proposed method

$$E_i - E_{pcc} = \left(\frac{X_i}{E_n}\right) Q_i \tag{5}$$

where E_i and E_{pcc} are the voltage of DG unit i and the PCC voltage, respectively. X_i is the feeder reactance of DG unit i. Q_i is the output reactive power of DG unit i.

The first term improves the reactive power sharing. However, a slight drift in the output voltage was observed. Therefore, short-term coupling between the active and reactive power droops was introduced during the short compensation duration, reducing the effect of the first term. This coupling involves injecting a signal related to the reactive power-sharing error from the *Q-E* droop into the *P-ω* droop relationship, as shown in Fig. 2. This causes a small disturbance that mitigates the effect of the compensation process on the output voltages and power-sharing level and maintains their values within the strictly allowable limits.

3.2 Proposed compensation trigger system

The proposed method does not require communication links to commence the compensation. Instead, it is activated using the proposed local load change detector, which detects the load change in each DG unit locally by observing the output current. Fig. 4 shows a flowchart of the proposed compensation trigger system.

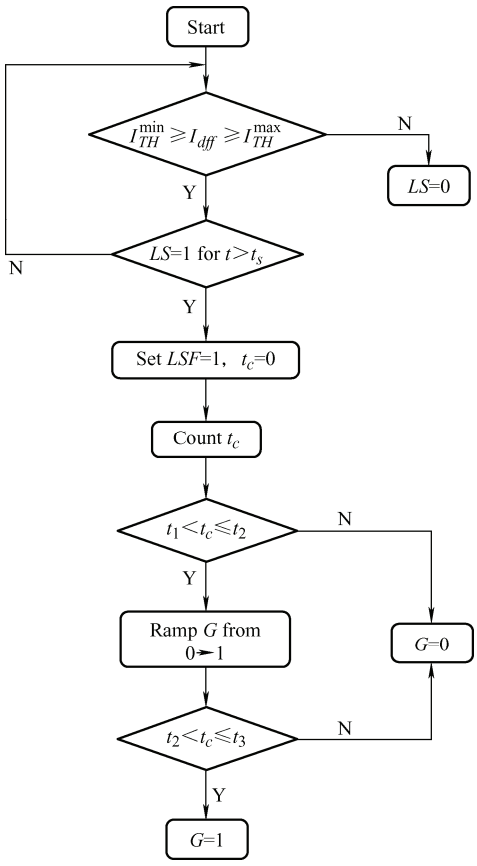

Fig. 4 Flow chart for the proposed compensation trigger system

To locally be able to detect any load change, the absolute value for the derivation of the DG output *d*-axis current (I_{df}) is passed through an LPF with a cut-off frequency of (ω_{df}). The absolute rate of change (I_{dff}) in Eq. (6) is used to detect load changes that occur in the network.

$$I_{df} = \frac{\omega}{s+\omega_{df}}\left|\frac{\mathrm{d}I_{df}}{\mathrm{d}t}\right| \tag{6}$$

If a load change is locally detected, the proposed compensation trigger system will check whether the load change is greater than or equal to a maximum predefined trigger value ($I_{TH}^{\max}$), which is set such that it is sufficiently high to not be falsely triggered by system noise and sufficiently low to detect any small change in the load. If a load change is detected to be greater than $I_{TH}^{\min}$, the system checks whether the load change lasts for a duration (t_s) long enough to be considered as a real system load change. If so, the timer (t_c) will reset to zero and the start time. A delay of t_1 is used to ensure that the system returns to steady state after detecting the load change. Finally, the compensation gain (G) gradually increases in milliseconds from ('0→ 1'), starting from t_1 to t_2. The purpose of not having a step change from ('0 to → 1') is to reduce the effect of additional terms on the droop relation. G was maintained at a value of '1' until compensation was completed at t_3.

The system was not reset unless the load change detected by the system was less than or equal to the minimum predefined trigger value ($I_{TH}^{\min}$). The purpose of having maximum and minimum predefined trigger values is to ensure that the system is not falsely detected with system noise and that the detected load change is an actual load change that requires a compensation process.

4 Small signal analysis and modeling

Small-signal analysis was employed to investigate the stability and transient performance of the proposed droop-control method. The active and reactive power flows for a DG unit in an isolated MG system are expressed as

$$P = \frac{1}{R^2+X^2}(RE^2 - REV\cos\delta + XEV\sin\delta) \tag{7}$$

$$Q = \frac{1}{R^2+X^2}(XE^2 - XEV\cos\delta - REV\sin\delta) \tag{8}$$

Considering the small variations in Eqs. (7) and (8), according to the DG voltage disturbances

$$\Delta P = \left(\frac{\partial P}{\partial \delta}\right)\Delta\delta + \left(\frac{\partial P}{\partial E}\right)\Delta E = k_{p\delta}\Delta\delta + k_{pE}\Delta E \tag{9}$$

$$\Delta Q = \left(\frac{\partial Q}{\partial \delta}\right)\Delta\delta + \left(\frac{\partial Q}{\partial E}\right)\Delta E = k_{q\delta}\Delta\delta + k_{qE}\Delta E \tag{10}$$

where Δ denotes perturbation around the operating point. $k_{p\delta}$, k_{pE}, $k_{q\delta}$, and k_{qE} are the real/reactive power flow sensitivities to the power angle (δ) and voltage magnitude (E), respectively.

Considering the small variations in the control method proposed in Eq. (3) and Eq. (4), the small-signal model for the proposed method can be expressed as

$$\Delta P_f = \frac{1}{\tau s+1}\Delta P \tag{11}$$

$$\Delta Q_f = \frac{1}{\tau s+1}\Delta Q \tag{12}$$

$$\Delta\omega = s\Delta\delta = -k_p\Delta P_f - k_s\Delta Q_f \tag{13}$$

$$\Delta E = -k_q\Delta Q_f - \left(\frac{k_c}{s}\right)\Delta Q_f \tag{14}$$

where τ is the LPF time constant.

By substituting Eq. (11) and Eq. (12) into Eq. (13) and Eq. (14), the dynamic performance of a DG unit during compensation using the proposed method can be described as

$$\left[\boldsymbol{A}(s) - \boldsymbol{B}(s)\boldsymbol{C}(s)\right]\left[\Delta\delta, \Delta E\right]^{\mathrm{T}} = 0 \tag{15}$$

where

$$\boldsymbol{A}(s) = \begin{pmatrix} s(\tau s+1) & 0 \\ 0 & s(\tau s+1) \end{pmatrix} \tag{16}$$

$$\boldsymbol{B}(s) = \begin{pmatrix} -k_p & -k_s \\ 0 & -sk_q - k_c \end{pmatrix} \tag{17}$$

$$\boldsymbol{C}(s) = \begin{pmatrix} k_{p\delta} & k_{pE} \\ k_{q\delta} & k_{qE} \end{pmatrix} \tag{18}$$

Finally, the closed-loop characteristic equation for the proposed method is obtained as

$$s^4\Delta\delta + As^3\Delta\delta + Bs^2\Delta\delta + Cs\Delta\delta + D\Delta\delta = 0 \tag{19}$$

where A, B, C, and D are defined as

$$A=\frac{2\tau+\tau k_q k_{qE}}{\tau^2} \tag{20}$$

$$B=\frac{k_q k_{qE}+k_c k_{qE}\tau+k_p k_{p\delta}\tau+k_s k_{q\delta}\tau+1}{\tau^2} \tag{21}$$

$$C=\frac{k_c k_{qE}+k_p k_{p\delta}+k_s k_{q\delta}+k_p k_{p\delta} k_q k_{qE}-k_p k_{pE} k_q k_{q\delta}}{\tau^2} \tag{22}$$

$$D=\frac{k_p k_{p\delta} k_c k_{qE}-k_p k_{pE} k_c k_{q\delta}}{\tau^2} \tag{23}$$

If the compensation parameters (k_c, k_s) are set to zero, the matrix in Eq. (15) represents the DG unit behavior using conventional droop control, as shown in Eqs. (1)-(2). Accordingly, the system becomes a third-order system.

$$\boldsymbol{B}(s)=\begin{pmatrix}-k_p & 0\\ 0 & -sk_q\end{pmatrix} \tag{24}$$

The system performances using different control parameters are shown in Figs. 5-8. The parameters used for the stability calculations are listed in Tab. 1. The performance of the system before compensation (using the conventional droop control) is shown in Fig. 5. k_c and k_s are set to zero, the active power coefficient (k_p) is fixed, and the reactive power coefficient (k_q) is increased from 1×10^{-5} to 6×10^{-4}. The results in Fig. 5 show that the system was not sensitive to variations in k_q within the range of interest.

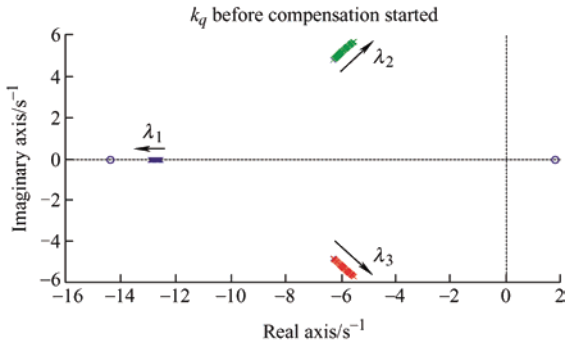

Fig. 5 Root locus for the system before the compensation process: k_p=1×10^{-4}, and 1×10^{-5} ⩽ k_q ⩽ 6×10^{-4}

During the compensation duration, two parameters were used for the compensation processes: k_c and k_s. Fig. 6 shows the performance of the system obtained by examining the effect of increasing k_q during the compensation processes (where the system becomes a fourth-order system). During the compensation duration and for the same variation range, the system becomes sensitive to k_q. However, to provide satisfactory system stability and damping performance, k_q was set to 2×10^{-5}. The sensitivity when k_c varies in the range of 5×10^{-4} to 5×10^{-3} while k_p, k_q, and k_s values are fixed is shown in Fig. 7.

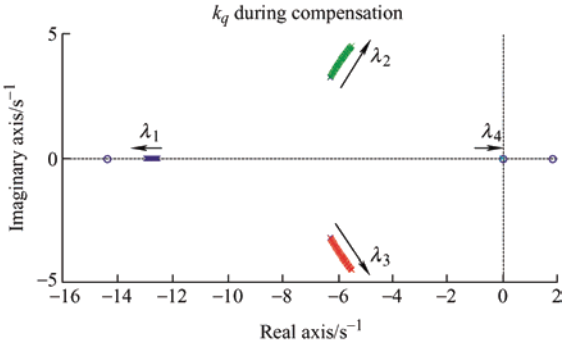

Fig. 6 Root locus for the system during the compensation process: k_p=1×10^{-4}, k_c=5.6×10^{-4}, k_s=1.7×10^{-5}, and 1×10^{-5} ⩽ k_q ⩽ 6×10^{-4}

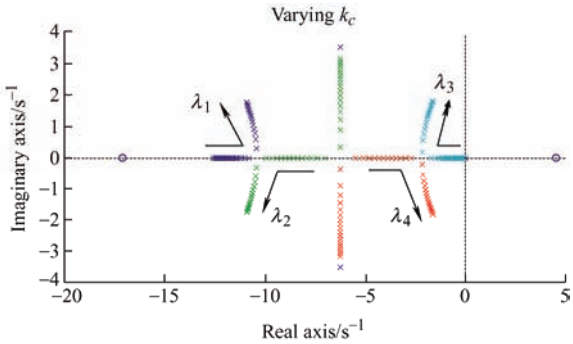

Fig. 7 Root locus for the system during the compensation process: k_p=1×10^{-4}, k_q=2×10^{-5}, k_s=1.7×10^{-5}, and 5×10^{-4} ⩽ k_c ⩽ 5×10^{-3}

Similarly, the performance of the system was evaluated using the dominant pole approximation. The system was not sensitive to variations in k_c. Fig. 8 shows the performance of the system when k_c increases from 1.5×10^{-5} to 8.8×10^{-5}, while k_p, k_q, and k_c are fixed. The results indicate that the system was stable throughout the range of interest. However, a high value of k_s can result in an unstable system. Accordingly, the parameters k_c and k_s should be sufficiently high to provide quick and accurate compensation. Meanwhile, they should be sufficiently low to maintain system stability. As a tradeoff, k_c was selected to be 5.6×10^{-4} and k_s to be 1.7×10^{-5}.

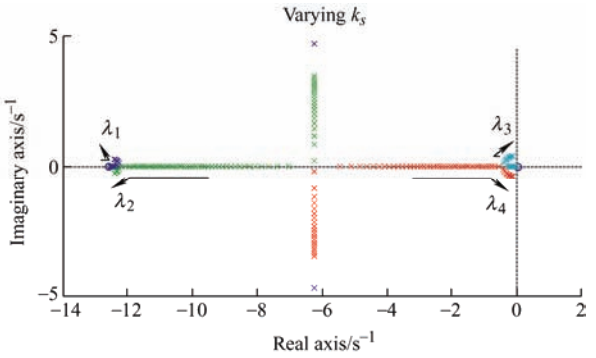

Fig. 8 Root locus for the system during the compensation process: k_p=1×10^{-4}, k_q=2×10^{-5}, k_c=5.6×10^{-4}, and 1.5×10^{-5} ⩽ k_s ⩽ 8.8×10^{-5}

Tab. 1 System parameters

Symbol		Value
Inverter parameters	L_f/mH	6.5
	C_f/μF	20
	f_n/Hz	50
	V_{DC}/V	800
	V_n/V	327
Network parameters	R_1, L_1	1 Ω, 1 mH
	R_2, L_2	1 Ω, 1 mH
	R_3, L_3	1 Ω, 1 mH
	R_{12}, L_{12}	0.25 Ω, 0.25 mH
	R_{23}, L_{23}	0.25 Ω, 0.25 mH
Load parameters	Load 1	10 kW, 5 kVar
	Load 2	10 kW, 5 kVar
	Load 3	10 kW, 5 kVar
	Local load	4.5 kW, 2 kVar
	$V_{ph\text{-}ph}$/V	400
Controller parameters	k_p/(rad/Wb)	1×10^{-4}
	k_q/(V/Var)	2×10^{-5}
	w_c, w_{df}/(rad/s)	12.56
	I_{TH}^{max}/(A/s)	10
	I_{TH}^{min}/(A/s)	4.3
	t_s/ms	10
	t_1, t_2, t_3/s	2, 2.3, 3
	k_c/(V/Var)	5.6×10^{-4}
	k_s/(V/Wb)	17×10^{-5}

5 Simulation results and discussion

To validate the effectiveness of the proposed system, the microgrid shown in Fig. 9, which consisted of three DGs, was simulated using Matlab/Simulink. The system parameters are listed in Tab. 1. The (R/X) ratio for the feeder impedance is chosen with a value of 3.2, representing a resistive microgrid system; hence, it is more challenging to provide accurate reactive power sharing. Furthermore, the values of (I_{TH} and t_s) were selected based on the response of the DG unit d-axis current for different load-step changes.

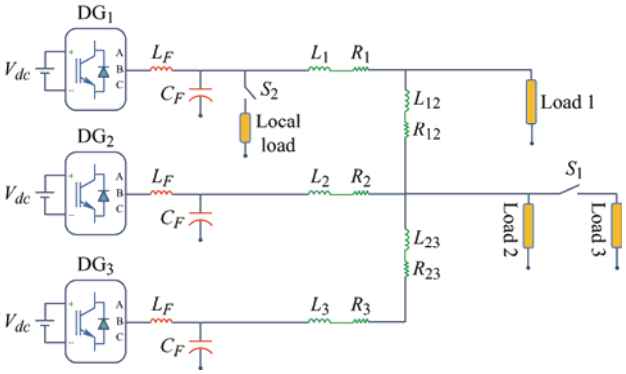

Fig. 9 Three DG microgrid system for the simulation

The performance of the proposed technique was validated by simulation using two case studies: load change (increase/decrease) and load change during compensation. The results of the proposed technique were compared with those of the conventional droop technique [4], represented by Eqs. (1) and (2), the method in Ref. [23], and the VSG technique in Ref. [26].

5.1 Operation of the proposed compensation trigger system

The process of the proposed compensation trigger system is illustrated in Fig. 9 as follows. Initially, all DG units operate with the conventional droop control; at 6 s, a load (load 3) is connected to the system, causing a load change that will be directly reflected to I_{dff} as shown in Figs. 10a and 10b. The flag signal LS is set to 1 when I_{dff} becomes greater than I_{TH}^{max}, as shown in Fig. 10c. Consequently, another flag signal, the LSF, is activated after a delay of t_s as shown in Fig. 10d. Finally, G will ramp from 0 to 1 during the duration t_1 = 8 s and t_2 = 8.3 s after a delay of 2 s to ensure that the system reaches the steady state before initiating the compensation process, as shown in Fig. 10e. The compensation process is activated for approximately 1 s (until t_3 = 9 s).

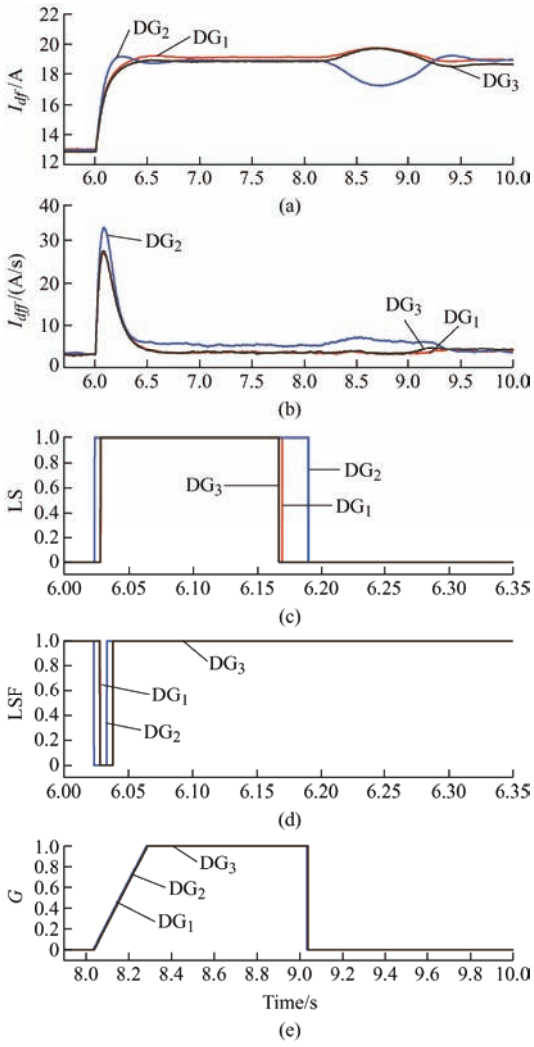

Fig. 10 Compensation flag trigger system

5.2 Load change at common bus

A change in the load at the common bus causes a change in the reactive power sharing, as shown in Fig. 11[4]. Therefore, this test verified that the proposed technique is immune to load changes on the common bus side. Initially, switch S_1 was opened, and the system connected two loads (loads 1 and 2) shared by three DG units, as shown in Fig. 9. At 6 s, S_1 was closed, and Load 3 was connected to the system. S_1 remains closed for 12 s. Power sharing for a conventional droop controller [4], the method in Ref. [23], VSG [26], and the proposed method were simulated and observed for a test duration of 20 s. The results are summarized in Tab. 2. The percentage reactive power-sharing error was calculated as

$$Q_{i,err}(\%) = \left(\frac{Q_{i,f} - Q_{i,exp}}{Q_{i,exp}} \right) \times 100 \tag{25}$$

where $Q_{i,exp}$ is the expected reactive power from DG_i.

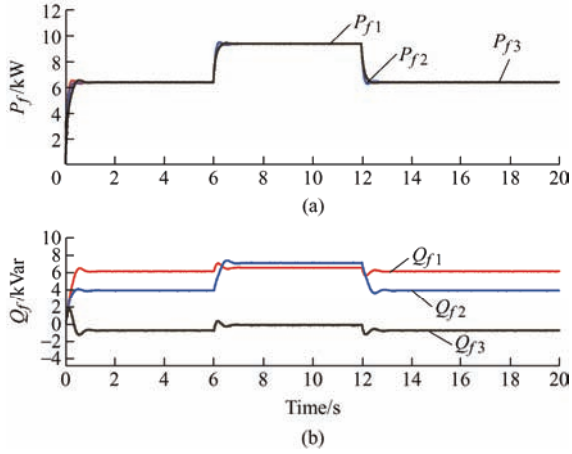

Fig. 11 Case 1: Power-sharing using the conventional method

Tab. 2 Simulation results for case studies 1 and 2

Case study		P/kW	Q_1/kVar	Q_2/kVar	Q_3/kVar	Q_{exp}/kVar	Q_{err}(%)	$V_{pu\text{-}1}$	$V_{pu\text{-}2}$	$V_{pu\text{-}3}$
S_1 open	Conv. [4]	6.44	6.18	3.95	–0.73	3.13	97.34, 25.92, –123.26	1.000	1.000	1.000
	Method in Ref. [23]	6.38	3.23	3.05	3.07	3.12	3.62, –2.19, –1.45	0.993	0.998	1.009
	VSG [26]	6.07	3.09	3.00	2.82	2.97	3.97, 1.01, –5.02	0.969	0.974	0.984
	Proposed	6.17	3.03	3.01	3.02	3.02	0.30, –0.13, –0.1	0.977	0.982	0.993
S_1 close	Conv. [4]	9.44	6.60	7.15	–0.10	4.55	45.12, 57.03, –102.23	1.000	1.000	1.000
	Method in Ref. [23]	9.36	4.86	4.66	4.06	4.53	7.41, 2.86, –10.24	0.995	0.995	1.009
	VSG [26]	9.05	4.19	4.74	4.19	4.37	–4.15, 8.29, –4.15	0.977	0.978	0.993
	Proposed	9.15	4.52	4.25	4.51	4.42	2.09, –4.01, 1.98	0.983	0.983	0.999
LCDS	Conv. [4]	6.44	6.18	3.94	–0.72	3.13	97.33, 25.74, –123.05	0.999	0.999	1.000
	Method in Ref. [23]	6.38	4.42	1.61	3.32	3.12	41.85, –48.45, 6.60	0.995	0.994	1.008
	VSG [26]	6.18	3.87	1.69	3.49	3.02	28.28, –43.96, 15.69	0.978	0.979	0.993
	Proposed	6.18	3.03	3.01	3.03	3.02	0.19, –0.51, 0.32	0.978	0.983	0.994

Power sharing using the method described in Ref. [23] is shown in Fig. 12. Using this method, Q_{err}(%) was reduced compared to the conventional droop, as listed in Tab. 2. In Fig. 13, power sharing using the VSG method [26] is shown. The VSG provides a quick response with a lower Q_{err}(%). Although the nominal output voltage is still within the allowable limits, the voltage level is affected more than that by the method in Ref. [23]. Moreover, the error reduction level was insignificant compared to that in Ref. [23]. Power sharing using the proposed method is shown in Fig. 14. Q_{err}(%) was the lowest among all compared methods, and the nominal output voltage was maintained within the accepted range of ±5%.

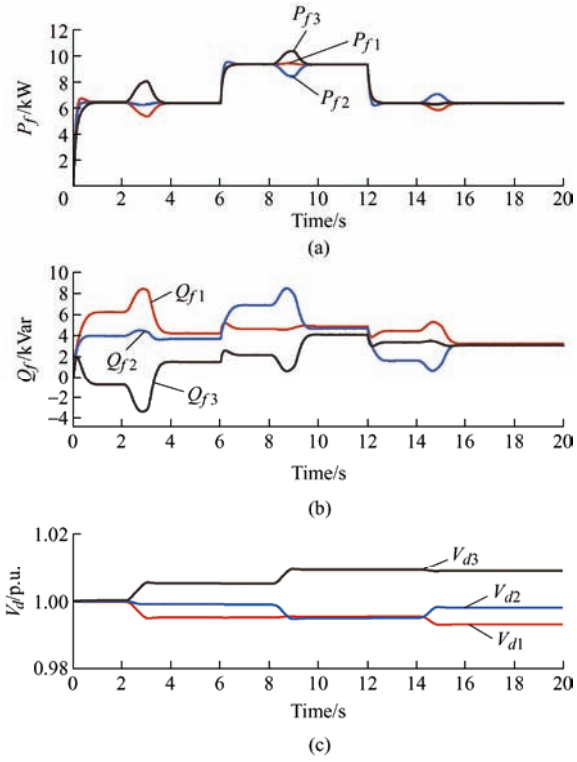

Fig. 12 Case 1: Power-sharing using the method in Ref. [23]

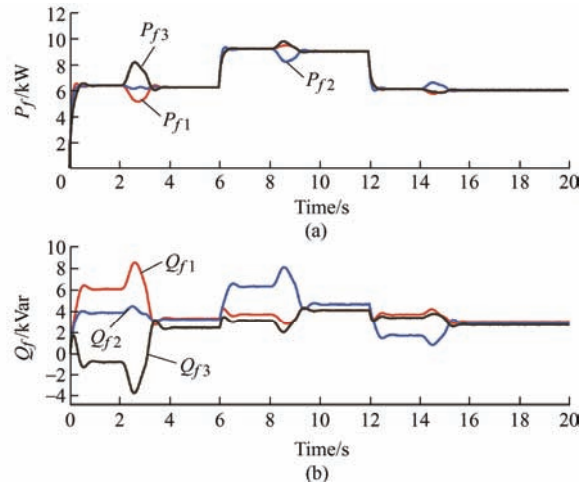

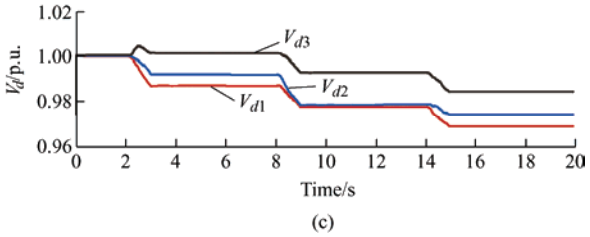

Fig. 13 Case 1: Power-sharing using the VSG method

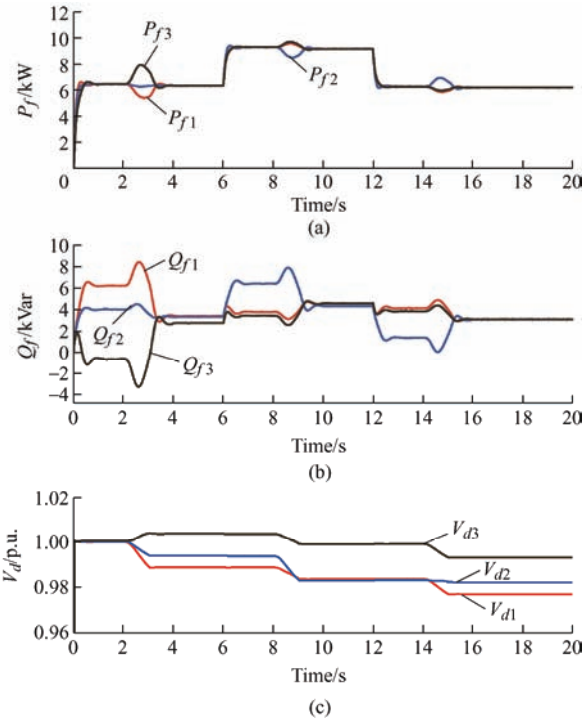

Fig. 14 Case 1: Power-sharing using the proposed method

Furthermore, Figs. 15 and 16 show the phase-a line currents of the three DG units before and after the

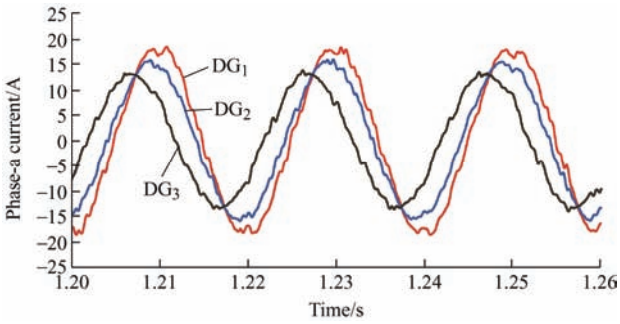

Fig. 15 Phase-a line currents before compensation

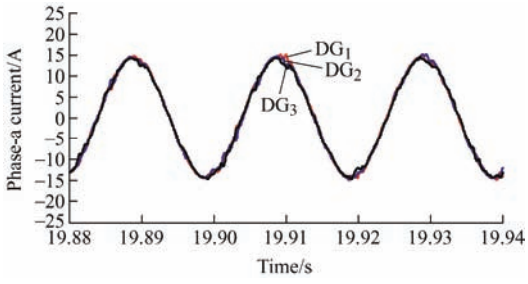

Fig. 16 Phase-a line currents after compensation using the proposed method

compensation process. The effectiveness of the proposed method is clear, as the currents for the three DGs after the compensation process are in phase.

5.3 Load change during compensation

The load change during compensation (LCDC) case was studied to highlight the robustness of the proposed method. Fig. 17 [4] illustrates the process sequence of this case study; S_1 is closed at 6 s, causing the trigger system to start the compensation processes at 8 s. S_1 is opened within the compensation duration. Power-sharing using the proposed method and the methods in the comparison are shown in Figs. 18-20, and their results are summarized in Tab. 2.

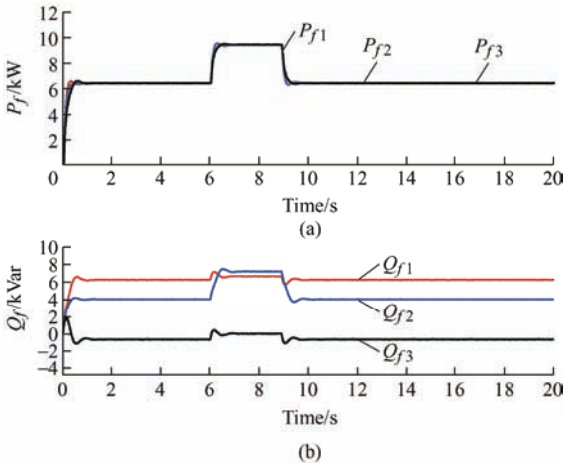

Fig. 17 Case 2: Power-sharing using the conventional method

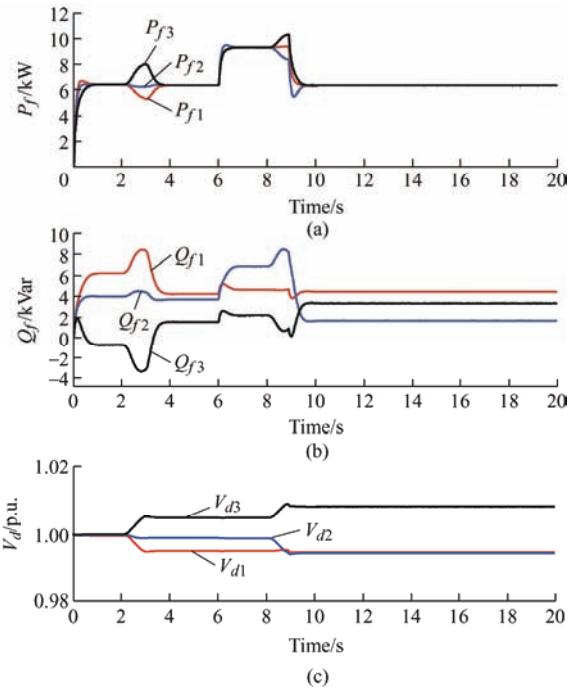

Fig. 18 Case 2: Power-sharing using the method in Ref. [23]

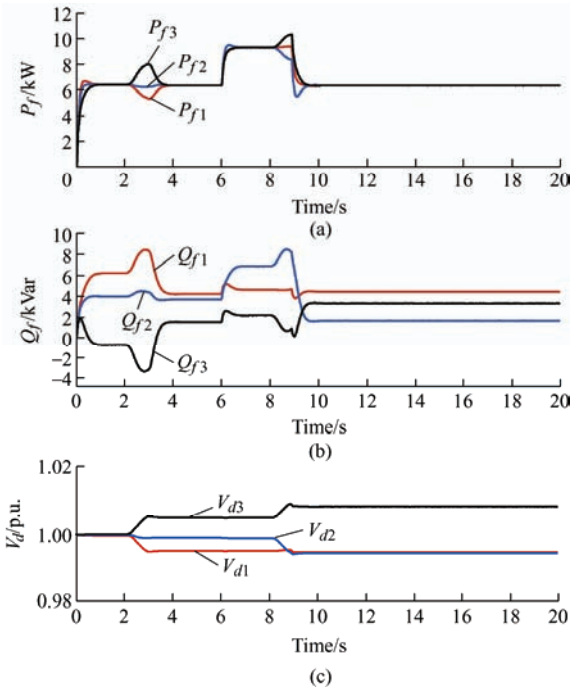

Fig. 19 Case 2: Power-sharing using the VSG method

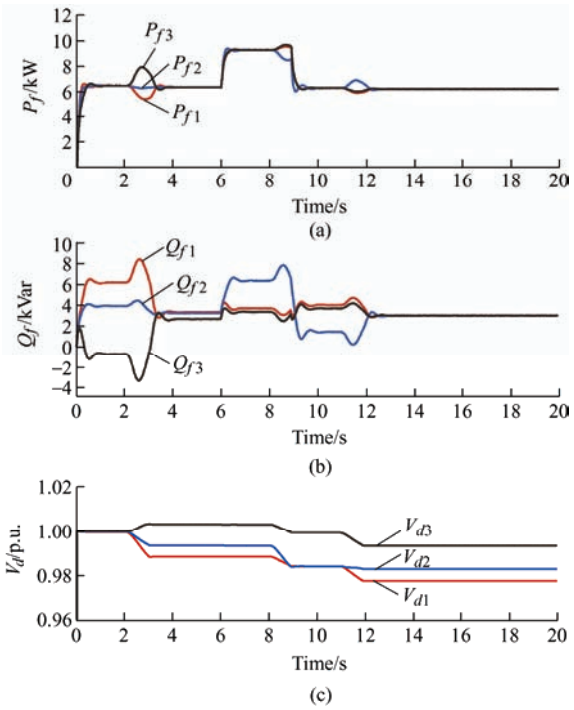

Fig. 20 Case 2: Power-sharing using the proposed method

From the results, the methods described in Ref. [23] and Ref. [26] cannot handle the case of LCDC because they cannot detect LCDC. However, the proposed method is effectively immune to the LCDC case because the proposed trigger system provides additional compensation to cancel any sharing errors caused by the LCDC.

5.4 Local load change

The existence of a local load further aggravates

reactive power-sharing mismatch. Fig. 21 shows the performance of the conventional method [4] when S_2 is closed at 6 s, thereby connecting a local load to the DG_1 side. S_2 remains closed until 12 s; then, the local load is disconnected.

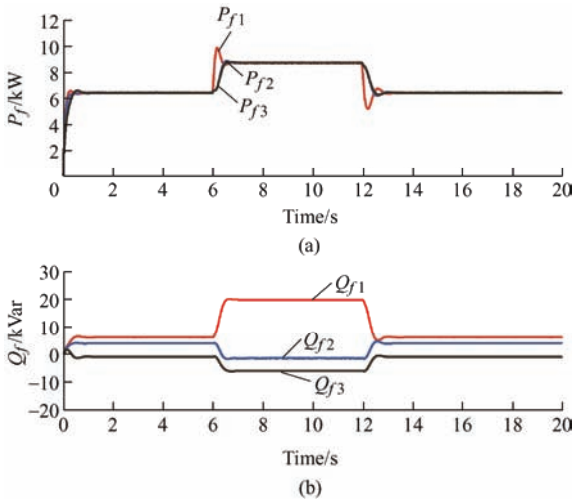

Fig. 21 Case 3: Local load change: Power-sharing using the conventional method

The power sharing of the proposed method is shown in Fig. 22, where the proposed trigger system detects the load change when the local load is connected to the system, activating the compensation process to cancel the reactive power-sharing mismatch. The results of the case study are listed in Tab. 3.

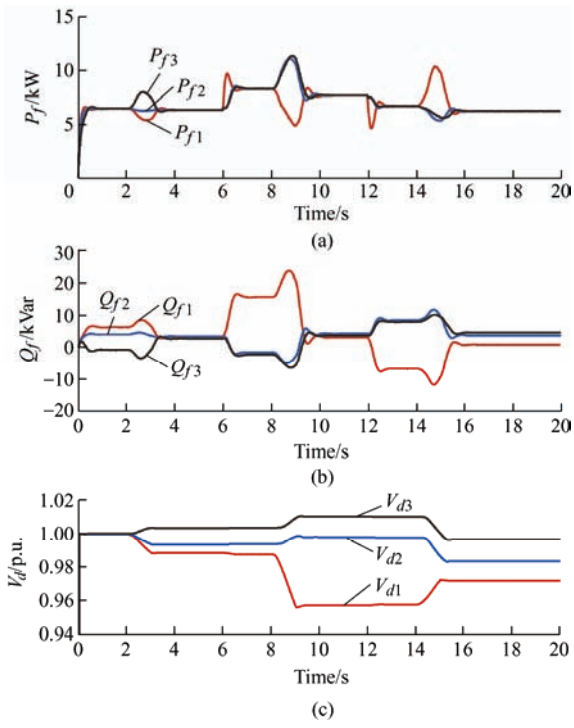

Fig. 22 Case 3: Local load change: Power-sharing using the proposed method

Tab. 3 Simulation results for case study 3

Case study		P/kW	Q_1/ kVar	Q_2 /kVar	Q_3 /kVar	Q_{exp}/kVar	Q_{err}(%)	$V_{pu\text{-}1}$	$V_{pu\text{-}2}$	$V_{pu\text{-}3}$
S_2 open	Conv. [4]	6.44	6.23	4.01	–0.84	3.13	98.84, 28.03, –126.85	1.000	1.000	1.000
	Proposed	6.20	0.84	3.69	4.54	3.02	–72.1, 22.08, 50.02	0.972	0.983	0.997
S_2 close	Conv. [4]	8.73	19.94	–1.35	–5.89	4.05	392.68, –133.36, –245.43	0.999	1.000	1.000
	Proposed	7.65	3.09	4.21	3.68	3.66	–15.55, 15.03, 0.55	0.957	0.998	1.010
Plug and play	Conv. [4]	6.44	6.24	4.01	–0.84	3.13	98.99, 27.91, –126.92	1.000	1.000	1.000
	Proposed	6.26	3.15	3.13	2.90	3.06	2.9, 2.31, –5.21	0.984	0.989	1.000

5.5 Plug and play feature

The method in Ref. [23] and the VSG method [26] are not plug-and-play methods owing to the involvement of a central controller. However, the proposed method offers plug-and-play features. To validate this claim, DG_3 is synchronized with the network at 6 s. The proposed trigger system detects the synchronizing event and provides a compensation process of approximately 8 s to cancel the resulting reactive power-sharing mismatch, as shown in Fig. 23. The results of this case study are summarized in Tab. 3.

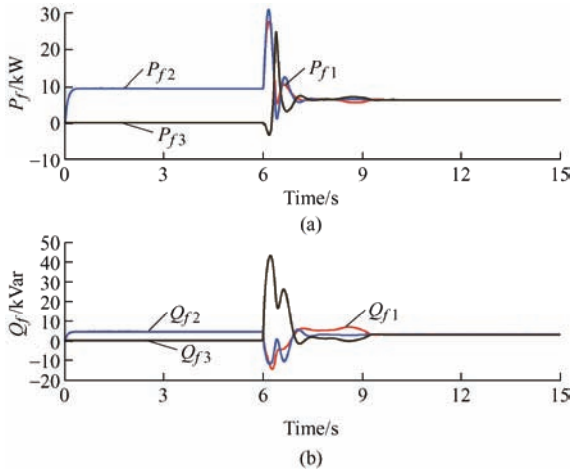

Fig. 23 DG_3 synchronizing using the proposed method

5.6 Design complexity and accuracy

Tab. 4 compares the design complexity based on additional component requirements, communication needs, and reactive power-sharing correction accuracy. The controller design described in Refs. [23, 26] required additional system components to implement a controller. Therefore, the controller design is complex. Moreover, a communication link is required from the central controller to simultaneously commence compensation for all the DG units. In Ref. [25], a local load detector is provided to cancel the need for a communication link used in Ref. [23]. This method uses the same controller as in Ref. [23], which has almost the same performance and design complexities as those in Ref. [23]. By contrast, the controller design for the proposed method is straightforward because it uses only compensator gains and integral action without extra dynamics. Furthermore, the need for a communication link from the central controller is eliminated by the proposed trigger system. The proposed method provided proportional reactive power sharing with a significantly low Q_{err}(%), as indicated by the simulation results and data in Tabs. 2 and 3.

Tab. 4 Design complexity and accuracy

Control method	Design complexity	Communication need	Power-sharing accuracy
Conv. [4]	N	N	Weak
Method in Ref. [23]	Y	Y	Strong
VSG [26]	Y	Y	Strong
Method in Ref. [25]	Y	N	Strong
Proposed	N	N	Superior

6 Conclusions

This study proposes a new method to reduce the reactive power-sharing error in an isolated microgrid system while maintaining the system parameters within their allowable limits. In the proposed method, the reactive power-sharing mismatch is reduced using a compensator term and integral action, which allows proportional reactive power sharing. Moreover, a small disturbance-carrying part of the error in the Q-E droop is inserted into the P-ω droop relation to mitigate the effect of the proposed reactive power sharing on the nominal output voltages without affecting any of the essential parameters of the system. In addition, a new compensation trigger system is proposed to commence the compensation process for all DG units simultaneously based on the local load-change detector, adding a plug-and-play feature to the proposed method.

References

[1] K Moslehi, R Kumar. A reliability perspective of the smart grid. *IEEE Transactions on Smart Grid*, 2010, 1(1): 57-64.

[2] X Huang, K Wang, J Qiu, et al. Decentralized control of multi-parallel grid-forming DGs in islanded microgrids for enhanced transient performance. *IEEE Access*, 2019, 7: 17958-17968.

[3] A Mehrizi-Sani, R Iravani. Potential-function based control of a microgrid in islanded and grid-connected modes. *IEEE Transactions on Power Systems*, 2010, 25(4): 1883-1891.

[4] M C Chandorkar, D M Divan, R Adapa. Control of parallel connected inverters in standalone AC supply systems. *IEEE Transactions on Industry Applications*, 1993, 29(1): 136-143.

[5] J Rocabert, A Luna, F Blaabjerg, et al. Control of power converters in AC microgrids. *IEEE Transactions on Power Electronics*, 2012, 27(11): 4734-4749.

[6] S Haider, G Li, K Wang. A dual control strategy for power sharing improvement in islanded mode of AC microgrid. *Protection and Control of Modern Power Systems*, 2018, 3(1): 1-8.

[7] Y Han, H Li, P Shen, et al. Review of active and reactive power sharing strategies in hierarchical controlled microgrids. *IEEE Transactions on Power Electronics*, 2016, 32(3): 2427-2451.

[8] K De Brabandere, B Bolsens, J Van den Keybus, et al. A voltage and frequency droop control method for parallel inverters. *IEEE Transactions on Power Electronics*, 2007, 22(4): 1107-1115.

[9] J M Guerrero, L G De Vicuna, J Matas, et al. A wireless controller to enhance dynamic performance of parallel inverters in distributed generation systems. *IEEE Transactions on Power Electronics*, 2004, 19(5): 1205-1213.

[10] Y Li, Y W Li. Power management of inverter interfaced autonomous microgrid based on virtual frequency-voltage frame. *IEEE Transactions on Smart Grid*, 2011, 2(1): 30-40.

[11] R Moslemi, J Mohammadpour. Accurate reactive power control of autonomous microgrids using an adaptive

virtual inductance loop. *Electric Power Systems Research*, 2015, 129: 142-149.

[12] J He, Y W Li. Analysis, design, and implementation of virtual impedance for power electronics interfaced distributed generation. *IEEE Transactions on Industry Applications*, 2011, 47(6): 2525-2538.

[13] L Lin, H Ma, Z Bai. An improved proportional load-sharing strategy for meshed parallel inverters system with complex impedances. *IEEE Transactions on Power Electronics*, 2016, 32(9): 7338-7351.

[14] M Zhang, B Song, J Wang. Circulating current control strategy based on equivalent feeder for parallel inverters in islanded microgrid. *IEEE Transactions on Power Systems*, 2018, 34(1): 595-605.

[15] M Shi, X Chen, J Zhou, et al. PI-consensus based distributed control of AC microgrids. *IEEE Transactions on Power Systems*, 2019, 35(3): 2268-2278.

[16] Y Zhu, F Zhuo, F Wang, et al. A virtual impedance optimization method for reactive power sharing in networked microgrid. *IEEE Transactions on Power Electronics*, 2015, 31(4): 2890-2904.

[17] Z Shuai, S Mo, J Wang, et al. Droop control method for load share and voltage regulation in high-voltage microgrids. *Journal of Modern Power Systems and Clean Energy*, 2016, 4(1): 76-86.

[18] D K Dheer, Y Gupta, S Doolla. A self-adjusting droop control strategy to improve reactive power sharing in islanded microgrid. *IEEE Transactions on Sustainable Energy*, 2019, 11(3): 1624-1635.

[19] E Rokrok, M E H Golshan. Adaptive voltage droop scheme for voltage source converters in an islanded multibus microgrid. *IET Generation, Transmission & Distribution*, 2010, 4(5): 562-578.

[20] Y Gupta, K Chatterjee, S Doolla. A simple control scheme for improving reactive power sharing in islanded microgrid. *IEEE Transactions on Power Systems*, 2010, 35(4): 3158-3169.

[21] C T Lee, C C Chu, P T Cheng. A new droop control method for the autonomous operation of distributed energy resource interface converters. *IEEE Transactions on Power Electronics*, 2012, 28(4): 1980-1993.

[22] H Han, Y Liu, Y Sun, et al. An improved droop control strategy for reactive power sharing in islanded microgrid. *IEEE Transactions on Power Electronics*, 2014, 30(6): 3133-3141.

[23] J He, Y W Li. An enhanced microgrid load demand sharing strategy. *IEEE Transactions on Power Electronics*, 2012, 27(9): 3984-3995.

[24] K Sabzevari, S Karimi, F Khosravi, et al. A novel partial transient active-reactive power coupling method for reactive power sharing. *International Journal of Electrical Power & Energy Systems*, 2019, 113: 758-771.

[25] Y Gupta, N Parganiha, A K Rathore, et al. An improved reactive power sharing method for an islanded microgrid. *IEEE Transactions on Industry Applications*, 2021, 57(3): 2954-2963.

[26] S Albatran, H Al-shorman. Reactive power correction using virtual synchronous generator technique for droop-controlled voltage source inverters in islanded microgrid. *Energy Systems*, 2023, 14: 391-417.

[27] W Yao, M Chen, J Matas, et al. Design and analysis of the droop control method for parallel inverters considering the impact of the complex impedance on the power sharing. *IEEE Transactions on Industrial Electronics*, 2010, 58(2): 576-588.

Issam A. Smadi (Senior Member, IEEE) received the B.Sc. degree in Electrical Engineering from Engineering Technology College, Al Balqa Applied University, Amman, Jordan, in 2000, the M.Sc. degree in Electric Power and Control Engineering from the Jordan University of Science and Technology, Irbid, Jordan, in 2003, and the Ph.D. degree in Electrical and Computer Engineering from Yokohama National University, Yokohama, Japan, in 2009. From 2009 to 2011, he was a Postdoctoral Fellow with the Department of Electrical and Computer Engineering at Yokohama National University. From 2011 to 2013, he was a Researcher and Development Electrical Engineer with Fuji Electric Company, Ltd., Tokyo, Japan. Since 2013, he has been with the Electrical Engineering Department of Jordan University of Science and Technology. He was appointed as a Manager of the Department of Linking with Industry, Consultative Center for Science and Technology, from 2018 to 2019. Also, he has been the Department Chair of the Electrical Engineering Department of Jordan University of Science and Technology from 2019 to 2022. Currently, he is an Associate Professor. His research interests include integrating renewable energy in power systems, control in power electronics, dynamic state estimation, electric drives, power system dynamics, and control.

Luay I. Shehadeh received his B.Sc. degree in Electrical Engineering from Hashemite University, Zarqa, Jordan, in 2017, and a M.Sc. degree in Control and Power Engineering from Jordan University of Science and Technology, Irbid, Jordan, in 2022. His research interests include grid synchronization, power electronics, electrical power systems' stability and control, smart grid, and renewable energy generation systems. Since 2018, he has been with the Airport International Group, Amman, Jordan, as Electromechanical Engineer.